Supporting Information

O_2 Activation by Bis(imino)pyridine Iron(II)-Thiolate Complexes

Yosra M. Badiei, Maxime A. Siegler and David P. Goldberg*

Department of Chemistry, Johns Hopkins University, Baltimore, Maryland 21212

General Information. All reactions were carried out under an inert dry atmosphere of N_2 or Ar using a drybox or standard Schlenk techniques. Dioxygen gas (2.6 Grade) was purchased from BOC Gases and dried by passage through a column of Drierite. $^{18}O_2$ (98%) was purchased from ICON (Isotope) Services, Inc., and $H_2{}^{18}O$ (95%) was purchased from Cambridge Isotope Laboratories, Inc. Iron(II) trifluoromethanesulfonate (98%) and Iron(II) dichloride (98%) was purchased from Sigma-Aldrich and Strem Chemicals Inc. respectively. Thiophenol (97%) and 2,6-diisopropylaniline (92%) was purchased from Acros. 2,6-diacetylpyridine (99%) was purchased from Sigma-Aldrich. All other reagents were purchased from commercial vendors and used without further purification unless noted otherwise. Diethyl ether and dichloromethane were purified via a Pure-Solv Solvent Purification System from Innovative Technology, Inc. THF was distilled from sodium/benzophenone. All solvents were degassed by repeated cycles of freeze-pump-thaw and then stored in a drybox. Acetonitrile was distilled over CaH_2. All solvents were degassed by repeated cycles of freeze-pump-thaw and then stored in a drybox. Sodium hydride (60% in mineral oil) was washed with hexanes prior to use. The bis(imino)pyridyl ($^{i\text{Pr}}$BIP) ligand 2,6-bis[1-(2,6-diisopropylphenylimido)ethyl]pyridine[1], [($^{i\text{Pr}}$BIP)$Fe^{II}(Cl)_2$] (**5**)[1] and [($^{i\text{Pr}}$BIP)$Fe^{II}(OTf)_2$] (**6**)[2] were synthesized according to literature procedures.

Instrumentation. ^{1}H-NMR spectra were recorded on a Bruker Avance 400 MHz NMR spectrometer at 298 K. All spectra were recorded in 5-mm o.d. NMR tubes, and chemical shifts were reported as δ values from standard solvent peaks. UV-visible spectra were recorded on a Varian Cary 50 Bio spectrophotometer. Electron paramagnetic resonance (EPR) spectra were obtained on a Bruker EMX EPR spectrometer controlled with a

Bruker ER 041 X G microwave bridge at 15 K. The EPR spectrometer was equipped with a continuous-flow liquid He cryostat and an ITC503 temperature controller made by Oxford Instruments, Inc. Cyclic voltammograms were measured with an EG&G Princeton Applied Research potentiostat/galvanostat model 263A with a three-electrode system consisting of a glassy carbon working electrode, a Ag/AgCl reference electrode (3.5 M KCl), and a platinum wire counter electrode. Measurements were performed with 0.10 M tetra-*n*-butylammonium hexaflurophosphate ($TBPF_6$) as the supporting electrolyte (purchased from Sigma-Aldrich Co., recrystallized from ethyl alcohol, and dried under vacuum prior to use) in dry CH_2Cl_2 at ambient temperatures under an inert nitrogen atmosphere. Potentials were calculated from $E_{1/2} = (E_{pa} + E_{pc})/2$ and were referenced to the ferrocenium/ferrocene couple (Fc^+/Fc).

Laser-desorption ionization mass spectrometry (LDIMS) was conducted on a Bruker Autoflex III TOF/TOF instrument equipped with a nitrogen laser at 335 nm using an MTP 384 ground steel target plate. LDIMS mass spectra were obtained in positive ion reflectron mode (LDIMS(+)), and LDI-TOF/TOF spectra were obtained in positive ion LIFT mode. Spectra were accumulated in multiples of 250 laser shots at a frequency of 200 Hz to a sum of 1000 shots total. Samples were deposited neat without the use of matrix. Electrospray ionization mass spectra (ESIMS) were collected on a Thermo Finnigan LCQ Duo ion-trap mass spectrometer fitted with an electrospray ionization source. The spray voltage was set at 5 kV and the capillary temperature was held at 250 °C. Gas chromatography (GC) was performed on an Agilent 6850 gas chromatograph fitted with a DB-5 5% phenylmethyl siloxane capillary column (30 m x 0.32 mm x 0.25 μm) and equipped with a flame-ionization detector. GC-MS was

performed on a Shimadzu GC-17A gas chromatograph fitted with a DB-5MS column and interfaced with a Shimadzu QP-5050A mass spectrometer. Analytical HPLC analyses were performed on an Agilent 1100 Series with a MetaChem Nucleosil C-18, 5 μm, 300 Å column. Elemental analyses were performed by Atlantic Microlab, Inc., Norcross, Georgia.

Synthesis of [($^{i\text{Pr}}$BIP)Fe$^{\text{II}}$(SPh)(Cl)] (**1**). In a 50 mL Schlenk flask, solid $NaSC_6H_5$ (0.09 g, 0.681 mmol) (prepared from addition of benzenethiol to NaH in THF) was added to a solution of [($^{i\text{Pr}}$BIP)Fe$^{\text{II}}$(Cl)$_2$] (0.400 g, 0.658 mmol) in THF (25 mL) and stirred for 3 h resulting in a dark blue solution. THF was removed under vacuum to give a dark blue/brown residue which was redissolved in CH_2Cl_2 (10 mL) and filtered through Celite to give a clear dark blue solution. The solution was concentrated to ca. half of the solvent volume and layered with a mixture of ether and pentane (2:1) and allowed to stand overnight in a – 35 °C freezer. Deep blue crystals were collected on a frit and dried to afford 0.200 g of **1**. The mother liquor was placed back in the freezer to yield a second crop of crystals (0.090 g) for a combined yield of 65% as a mono-CH_2Cl_2 solvate. Dark blue crystals suitable for X-ray diffraction were obtained after vapor diffusion with diethyl ether into a solution of **1** in CH_2Cl_2. UV-vis (CH_2Cl_2), λ_{max} 717 nm (3975 $M^{-1}cm^{-1}$). Magnetic susceptibility μ_{eff} (CD_2Cl_2, R.T.) = 5.2 μ_B. ^{1}H NMR (CD_2Cl_2): δ = 70.0 (s, 2H, Py-*H*$_m$), 24.7 (s, 2H, Ar-*H*$_p$), 17.6 (d, 5H, Ph-*H*), 3.5-2.3 (br, 12H, *i*-Pr-*Me*), -3.41-4.6 (br, 12H, *i*-Pr-*Me*), -5.3 (br, 2H, *i*-Pr-*Me*), -6.1 (s, 2H, Ar-*H*$_m$), -11.1 (s, 2H, Ar-*H*$_m$), -22.3 (s, 1H, Py-*H*$_p$), -25.1 (br s, 2H, *i*-Pr-C*H*), -43.1 (s, 6H, N=C(*Me*)). Note: Small quantities (< 5 %) of the starting material [($^{i\text{Pr}}$BIP)Fe$^{\text{II}}$(Cl)$_2$] (**5**) and disulfide PhS-SPh are often observed in the ^{1}H NMR spectrum of **1**. LDIMS(+): *m/z* 572.2 ([**1** – SPh]$^+$), 646.4

([**1** – Cl]$^+$). Anal. Calcd. for $C_{40}H_{50}Cl_3FeN_3S$ (**1**•CH_2Cl_2): C, 62.63; H, 6.57; N, 5.48. Found: C, 63.29; H, 6.66; N, 5.57.

Magnetic susceptibility measurements of 1. An NMR tube containing a solution of **1** (25 mM, 0.40 mL) was prepared with 25 μL tetramethylsilane (3%) in 0.75 μL of CD_2Cl_2 stock solution. An aliquot of this TMS solution (50 μL) in CD_2Cl_2 was transferred to a coaxial insert tube and was inserted into the NMR tube containing the iron solution. The shift of the TMS peak in the presence of the paramagnetic complex was compared to that of the TMS peak in the inner tube. The effective spin-only magnetic moment was calculated by simplified Evans method[3] using the equation, $\mu_{eff} = 0.0618(\Delta\nu T/2fM)^{1/2}$, where f is the oscillator frequency (MHz) of the superconducting spectrometer, T is the temperature (K), M is the molar concentration of the paramagnetic metal complex, and $\Delta\nu$ is the difference in frequency (Hz) between the two reference (TMS) signals. The number of unpaired electrons (n) was calculated using the following equation, $\mu^2 = n(n+2)$.

Synthesis of [($^{i\mathrm{Pr}}$BIP)Fe$^{\mathrm{II}}$(SPh)(OTf)] (**2**). To a solution of [($^{i\mathrm{Pr}}$BIP)Fe$^{\mathrm{II}}$(OTf)$_2$] (0.370 g, 0.443 mmol) in THF (15 mL) was added solid $NaSC_6H_5$ (0.064 g, 0.487 mmol, 1.1 equiv). The solution immediately turned forest green and was stirred for 1 h. THF was removed under vacuum to give a dark green/brown residue which was redissolved in CH_2Cl_2 (10 mL) and filtered through Celite to give a clear dark blue solution. The solution was concentrated to ca. half of the solvent volume and layered with pentane (3 mL) and allowed to stand overnight at -35 °C. Deep blue crystals were collected on a frit and dried

to afford 0.200 g (55 %) of **2**. ESIMS(+): *m/z* 686.3 ([**2** – SPh]$^+$), *m/z* 646.3 ([**2** – OTf]$^+$). UV-vis (CH_2Cl_2), λ_{max} 679 nm (3800 $M^{-1}cm^{-1}$). ^1H NMR (CD_2Cl_2): δ = 73.1, 49.5, 21.9, 15.3, 4.5, -1.59, -8.2, -33.0, -35.9, -55.3. ^1H NMR spectra of **2** have been observed to contain traces of [($^{i\text{Pr}}$BIP)$Fe^{II}(OTf)_2$] (**6**). Anal. Calcd. for $C_{40}H_{48}F_3FeN_3O_3S_2$: C, 60.37; H, 6.08; N, 5.28. Found C, 60.42; H, 6.20; N, 5.20.

Synthesis of [Fe^{II}($^{i\text{Pr}}$BIP)$(H_2O)_2(NCCH_3)$](OTf)$_2$ (7). (From aerobic oxidation of 2). To a solution of [($^{i\text{Pr}}$BIP)$Fe^{II}(OTf)_2$] (**6**) (0.200 g, 0.240 mmol) in MeCN (15 mL) was added solid $NaSC_6H_5$ (0.035 g, 0.264 mmol, 1.1 equiv). The solution immediately turned dark blue/brown and was stirred for 3 h. The solution was concentrated and the residue was redissolved in CH_2Cl_2 (10 mL) and filtered through Celite to give a clear dark blue solution. The CH_2Cl_2 solution was exposed to air and the solvent was allowed to evaporate slowly. Pink/red crystals were formed in 1 h to yield **7**. Complex **7** was found to be EPR silent (9.479 GHz, 15 K), consistent with an Fe(II) oxidation state. Anal. Calcd. for $C_{37}H_{50}F_6FeN_4O_8S_2$: C, 48.69; H, 5.52; N, 6.14. Found C, 48.97; H, 5.44; N, 5.31.

Reaction of [($^{i\text{Pr}}$BIP)Fe^{II}(SPh)(Cl)] (1) with O_2. In a typical reaction a solution of 10 mM **1** in dry CH_2Cl_2 (3 mL) was injected with dry O_2 (ca. 10 equiv.) and shaken vigorously. The solution was allowed to stir for 1 h and the color of the solution changed from dark blue to dark green over the course of the reaction. An aliquot of the reaction mixture was spotted immediately on to a MALDI target plate and the solvent was allowed to evaporate to dryness. Analysis by LDIMS(+) showed loss of the peak for the starting material **1** and an intense cluster at *m/z* 588.2, corresponding to

$[(^{i\text{Pr}}\text{BIP})\text{Fe}^{\text{IV}}(\text{O})(\text{Cl})]^+$ (**3**) (Figure S8). Tandem MS/MS experiments were consistent with the proposed structure of **3**. LDI-TOF/TOF for **3** (selected ion fragments; for complete spectrum see Figure S9): *m/z* 588.2 $[\mathbf{3}]^+$ (parent ion), *m/z* 572.2 ($[\mathbf{3} - \text{O}]^+$), *m/z* 552.7 ($[\mathbf{3} - \text{Cl}]^+$) (main fragment), *m/z* 536.5 $[(^{i\text{Pr}}\text{BIP})\text{Fe} - \text{H}^+]^+$, *m/z* 522.4 ($[(^{i\text{Pr}}\text{BIP})\text{Fe} - \text{Me}]^+$). The amount of disulfide PhS-SPh formed was quantitated by ^{1}H NMR giving 85% yield based on quantitation by integration against an internal standard (TMS). The same reaction performed with $^{18}\text{O}_2$ (98% ^{18}O) in place of $^{16}\text{O}_2$ gave a cluster centered at *m/z* 590.2 corresponding to $[(^{i\text{Pr}}\text{BIP})\text{Fe}^{\text{IV}}(^{18}\text{O})(\text{Cl})]^+$ (80% ^{18}O incorporation). For analysis by EPR, reaction mixtures were transferred directly to EPR tubes, and then sparged with Ar to remove any excess O_2 prior to slow annealing and storage at 77 K. X-band EPR spectra were collected at 15 K under non-saturating conditions. Typical parameters employed: frequency, 9.480 GHz; microwave power, 2 mW; modulation amplitude, 10 G; modulation frequency, 100 kHz; receiver gain, 5 x 10^3. Quantitation of the residual g= 4.3 signal (hs-Fe^{III}) was carried out by double-integration and comparison with a calibration curve constructed from a series of [(Fe^{III}(EDTA))]Na] – standard solutions (0.44, 0.88 and 4.4 mM). The hs-Fe^{III} signal accounted for < 5 % of the total iron content (3 independent samples).

Kinetic studies for the oxidation of PPh_3 to O=PPh_3 by 3. In a typical reaction, **3** was generated from the reaction of $[(^{i\text{Pr}}\text{BIP})\text{Fe}^{\text{II}}(\text{SPh})(\text{Cl})]$ (**1**) (1.5 x 10^{-4} M) and excess dry O_2 in CH_2Cl_2 in a quartz sealed cuvette. The solution was then sparged with Ar to remove excess O_2, and a solution of PPh_3 (50-300 equiv) dissolved in CH_2Cl_2 was added. The decay of **3** (green-brown) was monitored at 690 nm. The pseudo-first-order rate

constants, k_{obs}, were obtained by non-linear fitting of the decay in absorbance at 690 nm (Abs_{690}) versus time to the equation: ($Abs_t = Abs_f + (Abs_0 - Abs_f)\exp(-k_{obs}t)$), where Abs_f = final absorbance, Abs_0 = initial absorbance, A_t= absorbance at time t. A plot of k_{obs} vs [PPh_3] was linear and the slope of the best-fit line gave the second-order rate constant, k_2 (Figures S6 and S7).

Aerobic oxidation of PPh_3. An amount of [($^{i\text{Pr}}$BIP)Fe^{II}(SPh)(Cl)] (**1**) (0.020 g, 0.029 mmol) and 4 equiv. PPh_3 (0.031 g, 0.117 mmol) were dissolved in CD_2Cl_2 (0.7 mL) and transferred to a sealed NMR tube. The solution was frozen and the headspace was evacuated, and then dry O_2 (2.00 mL) was admitted to the headspace of the sealed tube via a syringe. The solution was allowed to warm to room temperature and the reaction was monitored by $^{31}P\{^1H\}$ NMR. After 30 min, O=PPh_3 was formed in 70 % ± 2 based on Fe(II). Reactions were run at least in triplicate.

Aerobic oxidation of PPh_3 in the presence of $H_2{}^{18}O$. An amount of [($^{i\text{Pr}}$BIP)Fe^{II}(SPh)(Cl)] (**1**) (0.010 g, 0.015 mmol) was dissolved in CH_2Cl_2 (3 mL) and O_2 (4 mL) was injected and the solution was allowed to stir for 1 h. The color of the solution changed from dark blue to dark green. The solution was frozen and the headspace was evacuated and filled with Ar, and then the solution was allowed to warm to room temperature. An amount of $H_2{}^{18}O$ (10 μL, 95% ^{18}O enriched) was added and the mixture was stirred for 5 min, after which time PPh_3 (0.015 mg, 0.057 mmol, 2 mL CH_2Cl_2) was added. The reaction mixture was stirred for 3 h and then analyzed by GC/MS, revealing the formation of $^{18}OPPh_3$ (50% ^{18}O incorporation).

Attempted reactions of [($^{i\text{Pr}}$BIP)$Fe^{II}(Cl)_2$] (5) or [($^{i\text{Pr}}$BIP)$Fe^{II}(OTf)_2$] (6) with O_2. In a typical reaction, **5** or **6** was dissolved in CH_2Cl_2, and the solution was saturated with dry O_2, and stirred for several days at room temperature. No reaction was observed by UV-vis, NMR, or mass spectrometry (LDIMS or ESIMS). Addition of excess PPh_3 to oxygenated solutions of **5** or **6** did not result in the formation of $O{=}PPh_3$ as monitored by ^{31}P NMR and GC-FID.

Reaction of [($^{i\text{Pr}}$BIP)Fe^{II}(SPh)(OTf)] (2) with O_2. In a typical reaction analyzed by mass spectrometry, a solution of 10 mM [($^{i\text{Pr}}$BIP)Fe^{II}(SPh)(OTf)] (0.038 mmol) in dry CH_2Cl_2 (3 mL) was injected with dry O_2 (ca. 5 equiv). A rapid color change was observed from dark blue to dark brown. After 15 min, an aliquot of the reaction mixture was spotted immediately to a MALDI target plate and the solvent was allowed to evaporate to dryness. Analysis by LDIMS(+) showed a cluster at *m/z* 694.42 corresponding to the triply-oxygenated cation $[Fe^{II}(^{i\text{Pr}}\text{BIP})(PhSO_3)]^+$. The analogous reaction performed with $^{18}O_2$ (98% ^{18}O) instead of $^{16}O_2$ gives *m/z* 700.45 corresponding to $[Fe^{II}(^{i\text{Pr}}\text{BIP})(PhS^{18}O_3)]^+$ (Figure S10). For reversed-phase HPLC, in a representative procedure, a solution of [($^{i\text{Pr}}$BIP)Fe^{II}(SPh)(OTf)] (0.02 g, 0.025 mmol) in dry CH_2Cl_2 (3 mL) was chilled at 0 °C to which ca. 10 equiv. of dry O_2 was injected. The solution rapidly changed color from dark blue to dark brown. The solution was stirred for 1 h. Two work-up procedures were followed: (1) A 1 M HCl solution (4 mL) was added and the biphasic mixture was vigorously stirred for 1 h (during which time the solution turned dark blue and then yellow). The aqueous layer was separated, filtered through Celite and

then an aliquot was directly injected onto the HPLC (95% H_2O, 5% CH_3CN, 0.1 % TFA). A major peak at 4.43 min was observed that matched that of an authentic sample of $PhSO_3H$. Quantitation of $PhSO_3H$ was performed by integration of the HPLC peak for $PhSO_3H$ and comparison with a calibration curve. Yield of $PhSO_3H$ (30 %) (based on **2**). (2) A base work-up was used to facilitate ^1H NMR analysis: 2 M NaOH (2 equiv.) was added to the reaction mixture of **2** and excess O_2 in CH_2Cl_2, and the biphasic mixture was filtered to remove a brown/orange precipitate. Extraction of the aqueous layer followed by lyophilization gave a white solid. The white solid was redissolved in D_2O and ^1H NMR analysis revealed the formation of the sulfonato product $PhSO_3H$ (δ 7.80, 7.57 ppm (pH = 8)). ESIMS(-) revealed a dominant ion at *m/z* = 157 corresponding to $PhSO_3^-$.

Cyclic voltammetry measurements

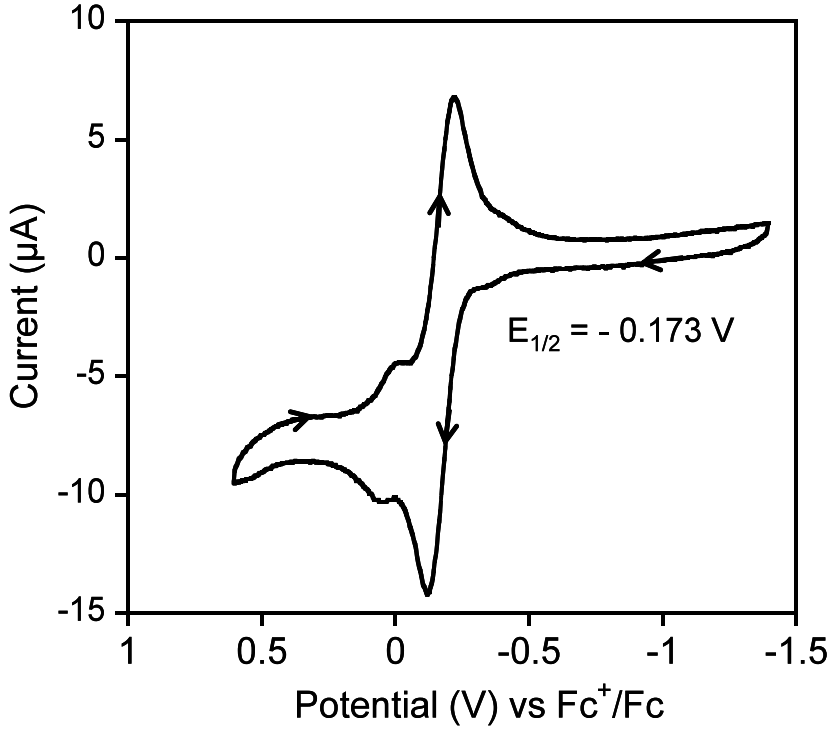

Figure S1. Cyclic voltammogram of complex **1 (**1.50 mM) in CH_2Cl_2 with 0.1 M TBAP as the supporting electrolyte; scan rate 100 mV s^{-1}. The small peak at $E_{1/2}$ = 0.023 V is assigned to a small amount of [($^{i\text{Pr}}$BIP)$Fe^{II}(Cl)_2$] (**5**) impurity ($E_{1/2}$ = 0.023 V, independent measurement).

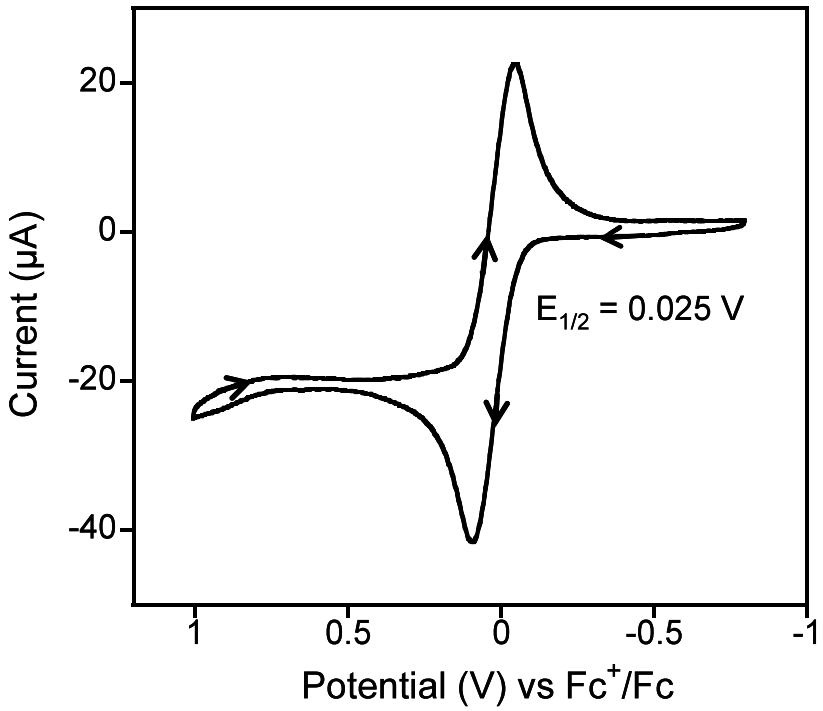

Figure S2. Cyclic voltammogram of complex **5 (**2.0 mM) in CH_2Cl_2 with 0.1 M TBAP as the supporting electrolyte, scan rate 100 mV s^{-1}.

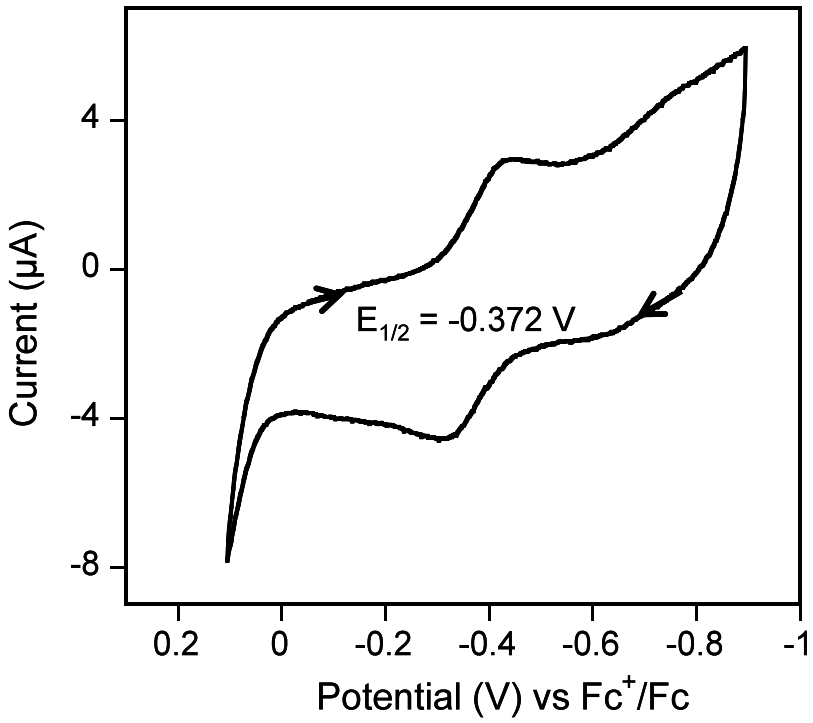

Figure S3. Cyclic voltammogram of complex **2 (**1.3 mM) in CH_2Cl_2 with 0.1 M TBAP as the supporting electrolyte, scan rate 100 mV s^{-1}.

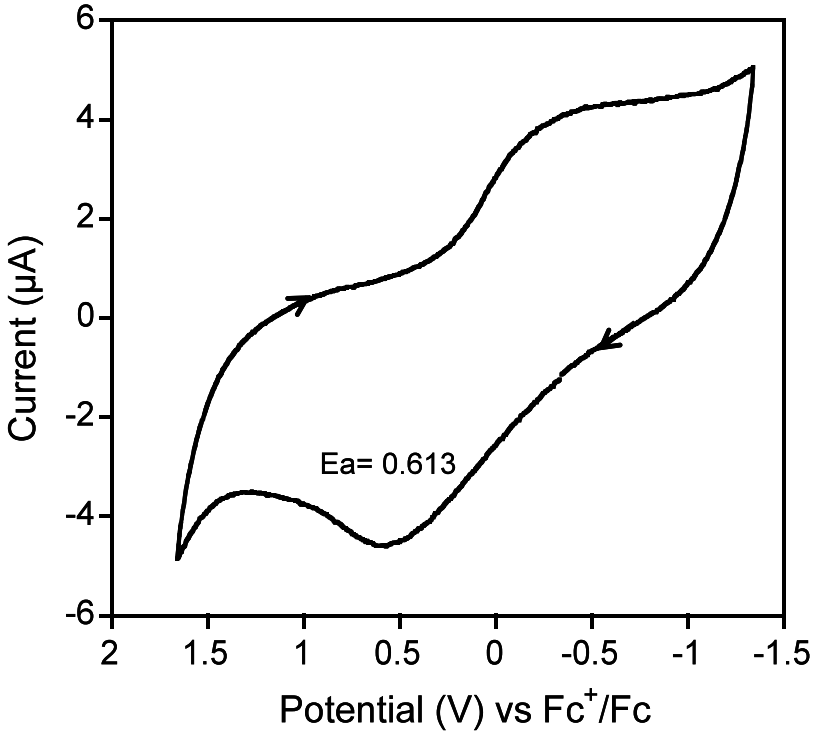

Figure S4. Cyclic voltammogram of **6** (2.9 mM) in CH_2Cl_2 with 0.1 M TBAP as the supporting electrolyte, scan rate 100 mV s^{-1}.

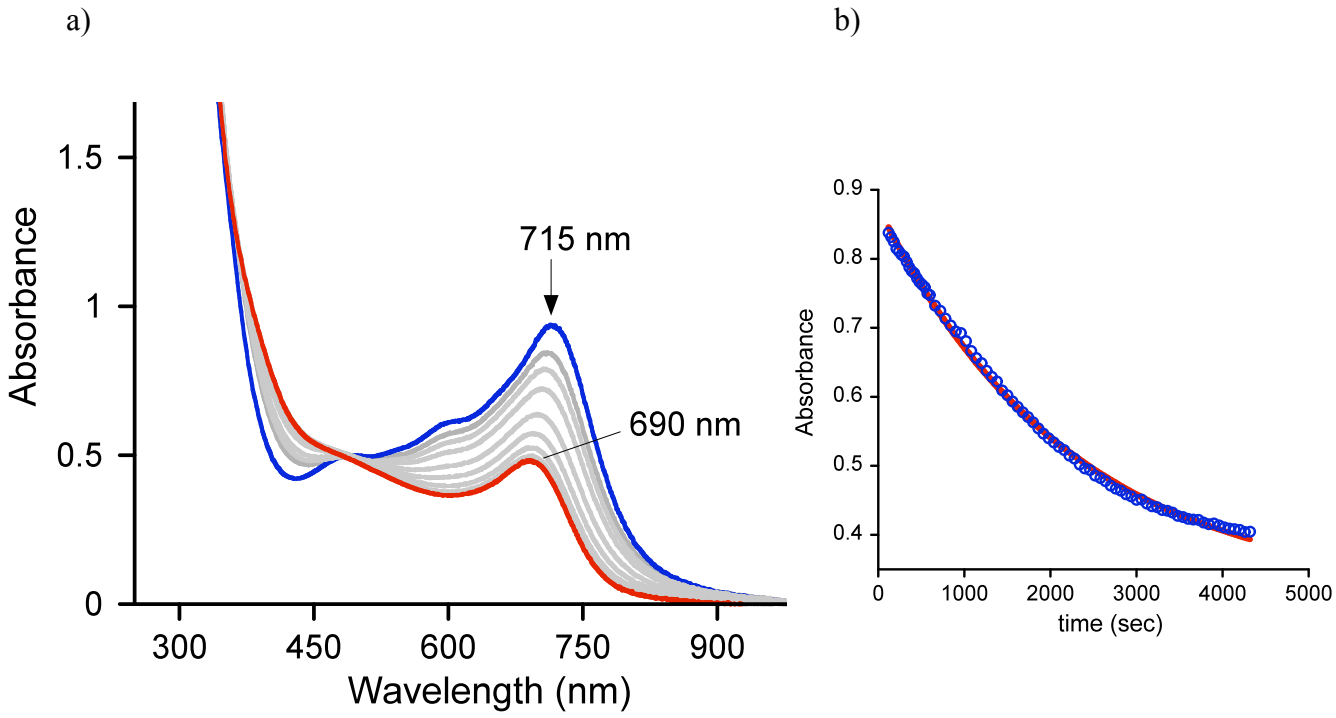

Figure S5. a) Time-resolved UV-vis spectra for the reaction of **1** (blue line) (715 nm, 0.23 mM) with excess O_2 in CH_2Cl_2 to give **3** (red line) (690 nm). b) Plot of A_{715} versus time (blue circles). A pseudo-first-order rate constant k_{obs} = 4 x 10^{-4} sec^{-1} ($t_{1/2}$ = 29 min) was obtained by non-linear least-squares fitting of the decay to the equation $Abs_t = Abs_f + (Abs_0 - Abs_f)exp(-k_{obs}t)$, where Abs_f = final absorbance, Abs_0 = initial absorbance, A_t = absorbance at time t. Best-fit line show in red.

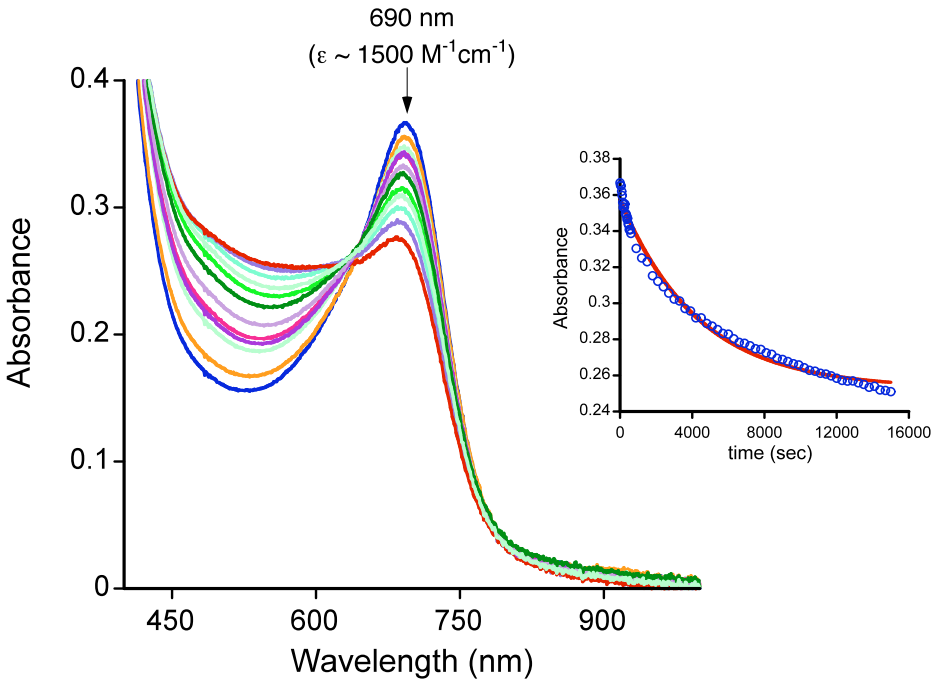

Figure S6. Time-resolved UV-vis spectra for the reaction of $[(^{i\text{Pr}}\text{BIP})\text{Fe}^{\text{IV}}(\text{O})(\text{Cl})]^{+}$ (**3**) with excess PPh_3 (100 equiv) in CH_2Cl_2 at 25 °C. Inset: Plot of A_{690} versus time (blue circles) and the best-fit line (red).

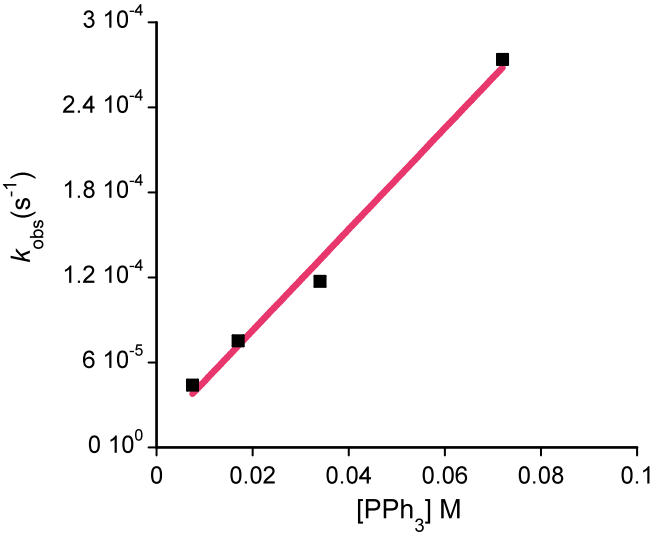

Figure S7. Plot of k_{obs} against PPh_3 concentrations. The slope of the best-fit line equals the apparent second-order rate constant ($k_2 = 3.6 \pm 0.3 \times 10^{-3}$ M^{-1} s^{-1}). $k_{obs} = k_2[PPh_3]$.

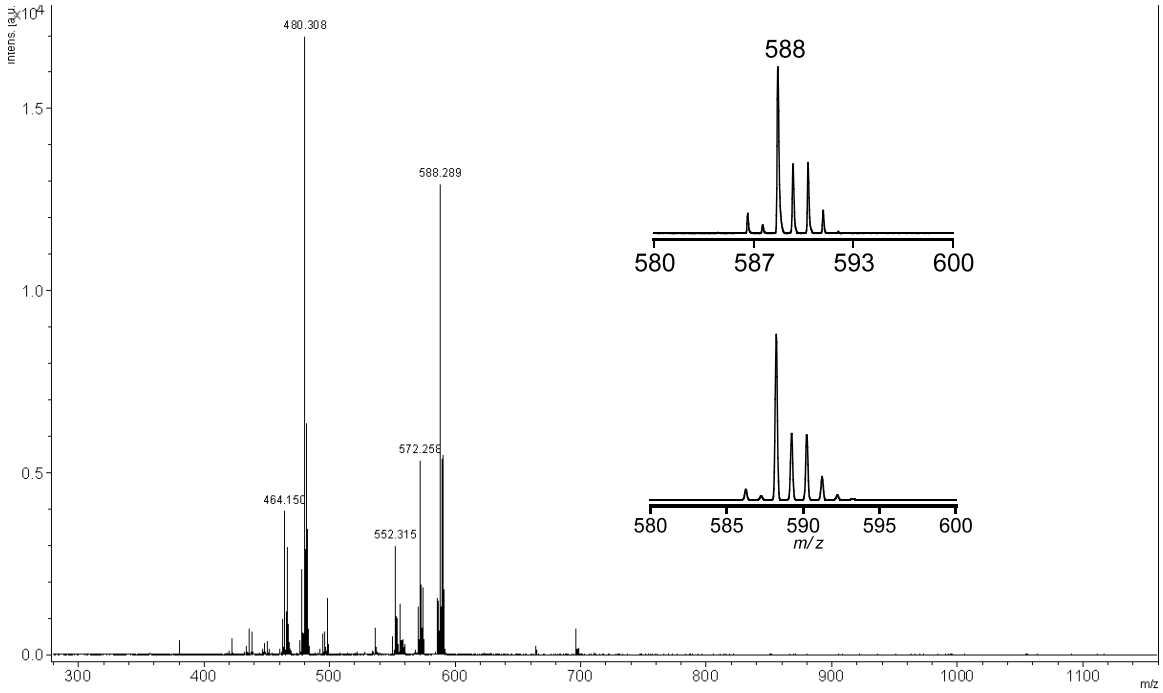

Figure S8. Full range LDI-TOFMS(+) of **1** + excess O_2 (10 equiv) after 1 h. The major peaks at *m/z* 588.29, 572.26, 480.31 correspond to $[(^{i\text{Pr}}\text{BIP})\text{Fe(O)(Cl)}]^+$ (**3**), $[\mathbf{3} - \text{O}]^+$ and free ligand ($^{i\text{Pr}}$BIP) respectively. Inset: Isotope distribution pattern for **3**. Top: exptl, bottom: calcd.

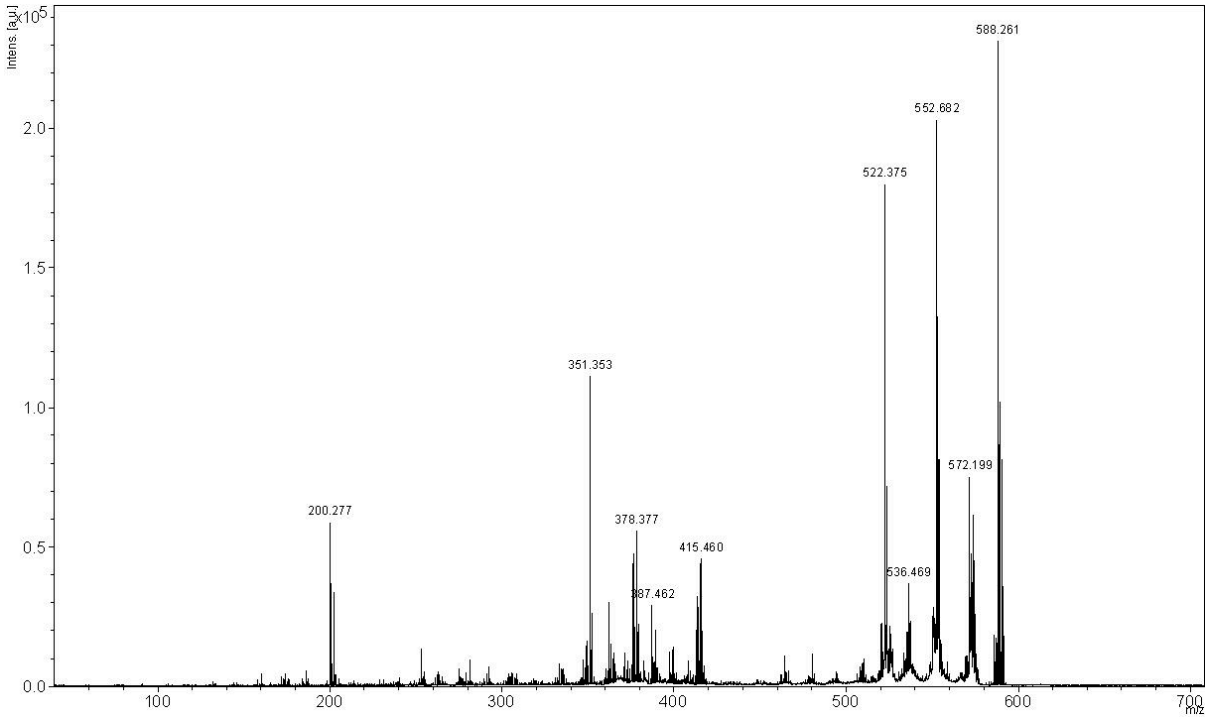

Figure S9. LDI-TOF/TOF spectra of **3**. Fragmentation of the peak at *m/z* 588 gives rise to the major fragments *m/z* 572.2 ([**3** - O]$^+$), *m/z* 552.7 ([**3** - Cl]$^+$) (main fragment), *m/z* 536.5 [($^{i\text{Pr}}$BIP)Fe – H]$^+$, *m/z* 522.4 ([($^{i\text{Pr}}$BIP)Fe - Me]$^+$).

.

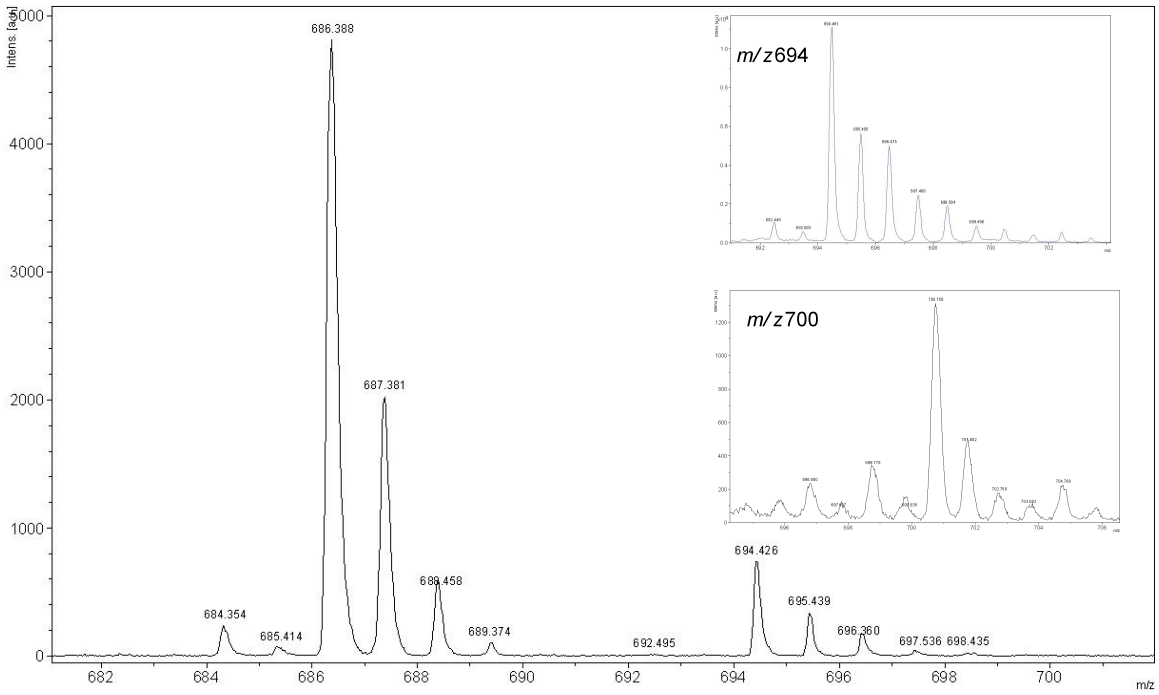

Figure S10. LDIMS(+) of **2** + excess O_2 (10 equiv) after 20 min. The major peaks at *m/z* 686.39 and 694.42 correspond to $[Fe^{II}(^{iPr}BIP)(OTf)]^+$ and $[Fe^{II}(^{iPr}BIP)(PhSO_3)]^+$ respectively. Inset: isotopic cluster for $[Fe^{II}(^{iPr}BIP)(PhSO_3)]^+$ prepared from $^{16}O_2$ (top) and $^{18}O_2$ (bottom).

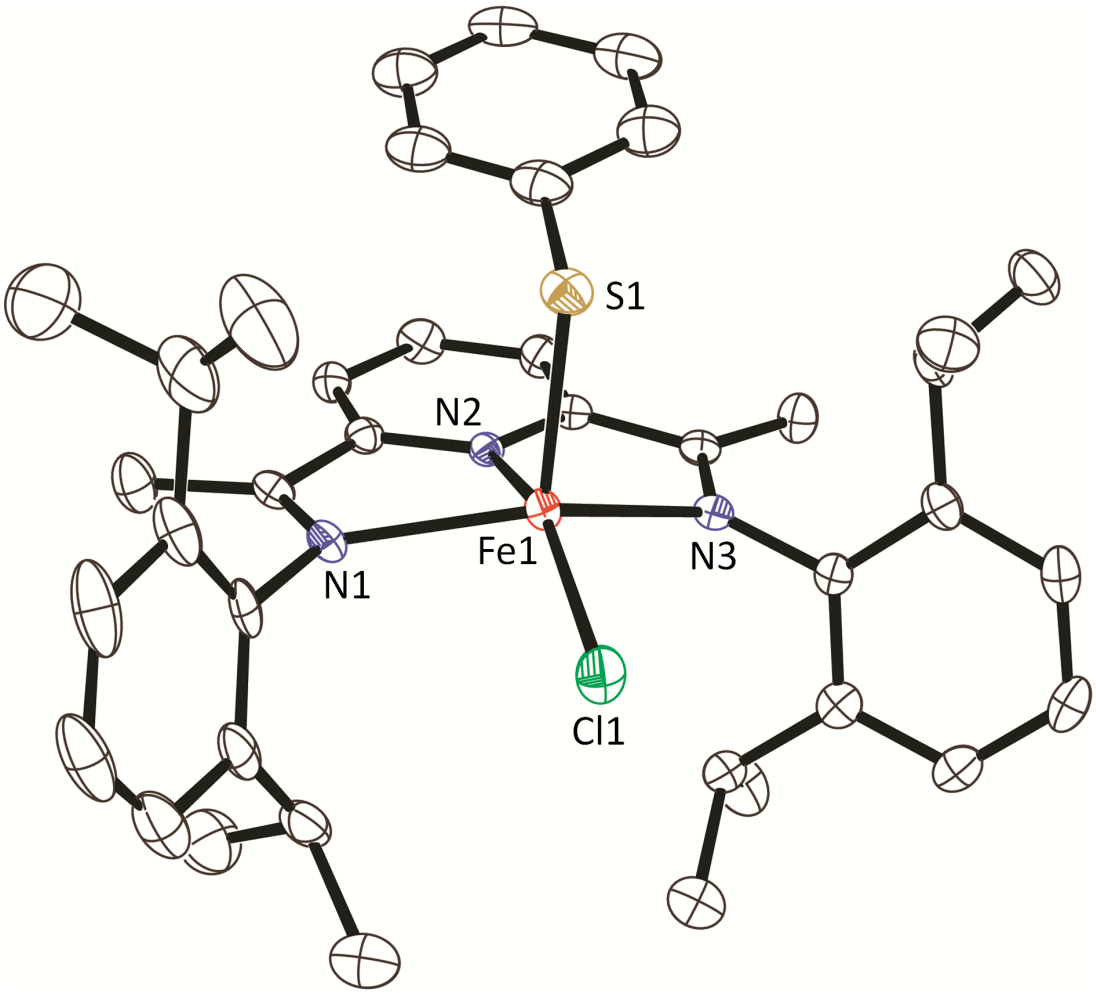

Figure S11. Displacement ellipsoid plots (50% probability level) of **1**. All H atoms are deleted for clarity. Selected bond distances (Å) and angles (°): Fe1-N1 2.212(2), Fe1-N2 2.054(2), Fe1-N3 2.192(2), Fe1-Cl1 2.2560(9), Fe1-S1 2.3305(9), N3-Fe1-N1 141.21(9), N2-Fe1-Cl1 153.21(7), N2-Fe1-N3 73.62(9), N2-Fe1-N1 73.64(9), N3-Fe1-Cl1 100.15(7), N1-Fe1-Cl1 99.72(7), N2-Fe1-S1 95.11(7), N1-Fe1-S1 104.32(7), Cl1-Fe1-S1 111.65(4).

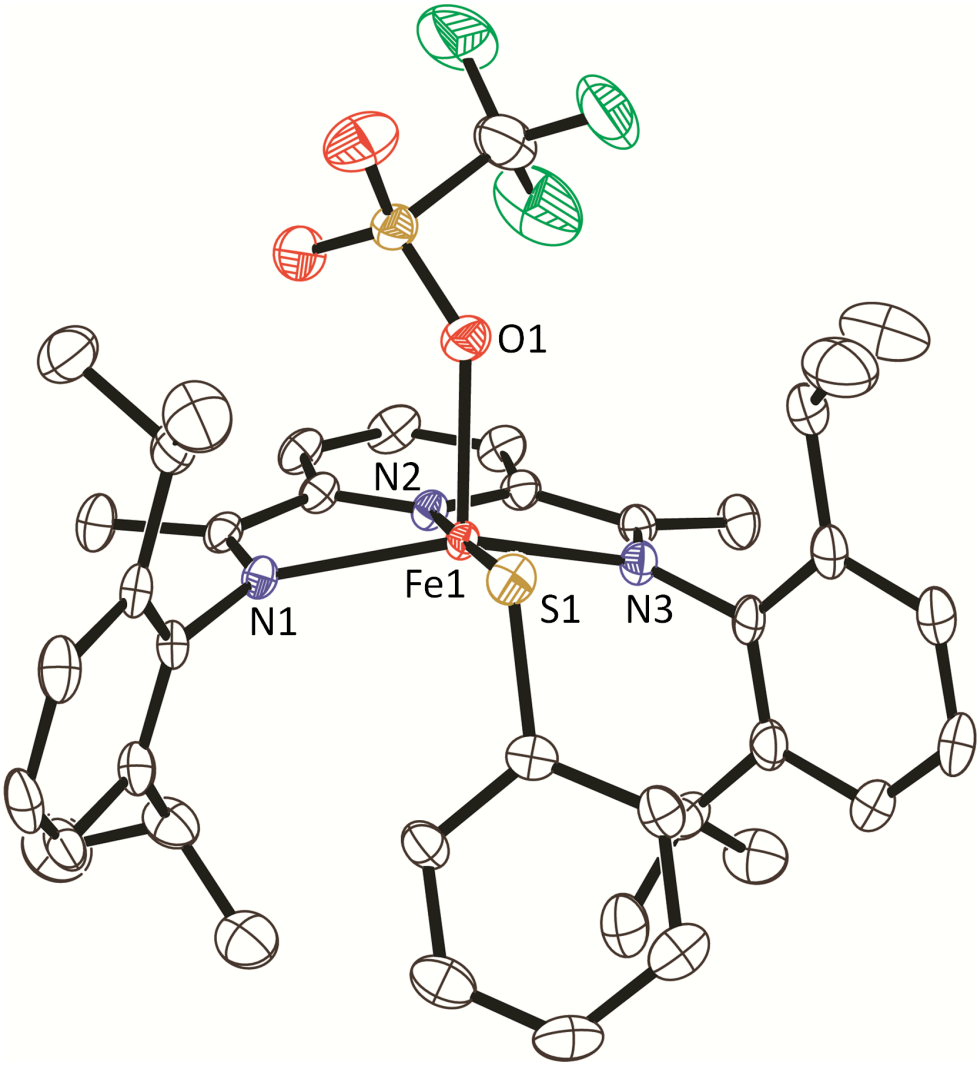

Figure S12. Displacement ellipsoid plots (50% probability level) of **2**. All H atoms are deleted for clarity. Selected bond distances (Å) and angles (°): Fe1-N1 2.238(2), Fe1-N2 2.091(2), Fe1-N3 2.208(2), Fe1-O1 2.1458(18), Fe1-S1 2.2795(9), N3-Fe1-N1 138.99(8), N2-Fe1-N1 72.93(8), N1-Fe1-S1 109.29(6), N2-Fe1-S1 177.52(7), N3-Fe1-S1 104.40(6), N1-Fe1-O1 102.18(7), N2-Fe1-O1 87.43(8), N3-Fe1-O1 98.59(7), N2-Fe1-N3 73.12(8), O1-Fe1-S1 93.09(6).

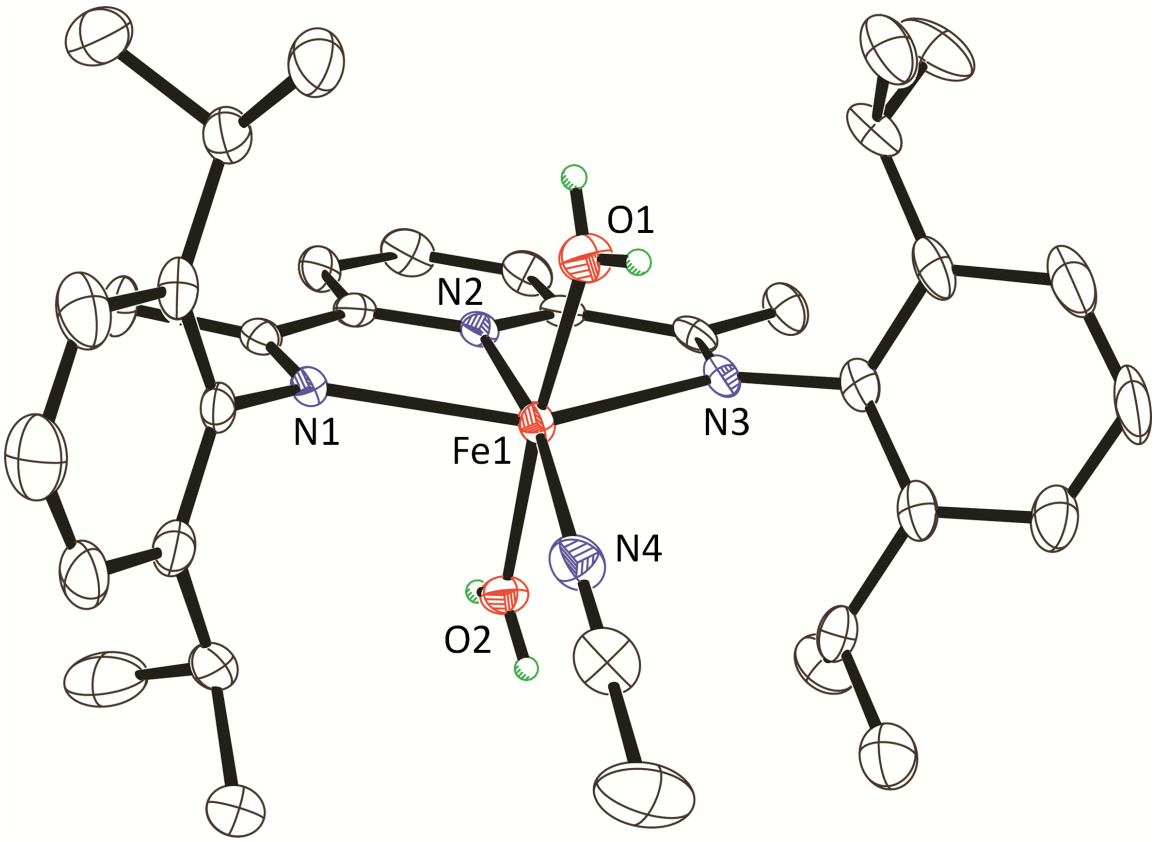

Figure S13. Displacement ellipsoid plots (50% probability level) of cationic **7**. The H atoms, the triflate counterions and CH_2Cl_2 molecule are omitted for clarity. Selected bond distances (Å) and angles (°): Fe1-O1 2.075(2), Fe1-O2 2.161(2), Fe1-N2 2.086(3), Fe1-N4 2.105(3), Fe1-N1 2.276(3), Fe1-N3 2.280(3), O1-Fe1-O2 173.40(10), O1-Fe1-N4 87.59(10), O1-Fe1-N1 92.22(10), O1-Fe1-N2 102.98(10), O1-Fe1-N3 87.74(10), N1-Fe1-N3 147.36(9), N2-Fe1-N3 74.03(10), N2-Fe1-N4 168.56(10), N2-Fe1-N1 74.20(10), N4-Fe1-N1 101.37(10), O2-Fe1-N1 91.97(9), N2-Fe1-O2 83.08(9), O2-Fe1-N4 86.58(10), N3-Fe1-N4 111.23(10), N3-Fe1-O2 91.48(9).

X-ray structure determination

General methods. All reflection intensities were measured at 110(2) K using a KM4/Xcalibur (detector: Sapphire3) with enhance graphite-monochromated Mo *K*α radiation (λ = 0.71073 Å) under the program CrysAlisPro (Version 1.171.33.31 for **1**, Version 1.171.33.48 for **2** and **7**, Oxford Diffraction Ltd., 2009). The program CrysAlisPro (Version 1.171.33.31 for **1**, Version 1.171.33.48 for **2** and **7**, Oxford Diffraction Ltd., 2009) was used to refine the cell dimensions. Data reduction was done using the program CrysAlis RED (Version 1.171.33.31 for **1**, Version 1.171.33.48 for **2** and **7**, Oxford Diffraction Ltd., 2009). The structures were solved with the program DIRDIF08[4] for **1** or with SHELXS-97 (Sheldrick, 2008)[5] for **2** and **7**, and were refined on F^2 with SHELXL-97 (Sheldrick, 2008). Analytical numeric absorption corrections based on a multifaceted crystal model were applied using CrysAlis RED (Version 1.171.33.31 for **1**, Version 1.171.33.48 for **2** and **7**, Oxford Diffraction Ltd., 2009). The temperature of the data collection was controlled using the system Cryojet (manufactured by Oxford Instruments). The H-atoms (except when specified) were placed at calculated positions using the instructions AFIX 13, AFIX 23 (for **1** and **7** only), AFIX 43 or AFIX 137 with isotropic displacement parameters having values 1.2 or 1.5 times *U*eq of the attached C atom. The coordinates of the H atoms of the two coordinated water molecules of complex **7** were restrained such that the O−H bond lengths and H−O−H angles have values within accepted ranges [*i.e.*, d(O−H) = 0.82−0.84 Å, d(H···H) ~ 1.32 Å so that H−O−H ~ 104.5º].

Complex **1.** The asymmetric unit of **1** contains one molecule of the Fe complex and one lattice dichloromethane molecule. The thiolate ligand is disordered over two positions, and the occupancy factor of the major component refines to 0.62(2). The absolute configuration was established by anomalous-dispersion effects in diffraction measurements on the crystal. The flack parameter refines to -0.002(14). Fw = 767.09, black octahedron, 0.38 × 0.24 × 0.20 mm^3, tetragonal, $P4_1$ (no. 76), a = 12.73727(14), c = 25.1972(4) Å, V = 4087.94(9) $Å^3$, Z = 4, D_x = 1.246 g cm^{-3}, μ = 0.646 mm^{-1}, abs. corr. range: 0.859–0.904. 23227 Reflections were measured up to a resolution of $(\sin \theta/\lambda)_{max}$ =

0.59 Å^{-1}. 7190 Reflections were unique (R_{int} = 0.0366), of which 6240 were observed [$I > 2\sigma(I)$]. 498 Parameters were refined with 184 restraints. $R1/wR2$ [$I > 2\sigma(I)$]: 0.0382/0.0908. $R1/wR2$ [all refl.]: 0.0463/0.0929. S = 1.016. Residual electron density found between −0.46 and 0.50 e Å^{-3}.

Complex **2.** Initial attempts at solving/refining the structure showed that some residual electron density peaks as high as 0.66-1.43 e Å^{-3} were found near the metal center and the thiolate ligand. The largest peak was found near the Fe center, which may suggest slight disorder of the metal center. The positions of the remaining residual peaks suggest the existence of a second coordinated triflate counterion (see Figure S14). The crystal that was mounted on the diffractometer is likely to be a phase mixture made of the target compound (*i.e.*, the Fe center is coordinated by the $^{i\text{Pr}}$BIP ligand, one triflate counterion and one thiolate ligand) and a small impurity of the starting material [($^{i\text{Pr}}$BIP)Fe(OTf)$_2$] (**6**). This observation is in agreement with the NMR data for **2** that show traces of **6**. For the particular crystal that was selected, the occupancies of the minor and major components refine to 8.3 and 91.7%, respectively. The atoms of the low-occupancy sites (the second triflate counterion) were refined isotropically. However, the amount of **6** in the bulk sample cannot be determined based on this refinement. Fw = 799.20, small dark brown block, 0.26 × 0.23 × 0.10 mm^3, monoclinic, $P2_1/c$ (no. 14), a = 12.7360(2), b = 18.3040(3), c = 17.2827(3) Å, β = 99.0194(17)º, V = 3979.12(11) Å^3, Z = 4, D_x = 1.334 g cm^{-3}, μ = 0.540 mm^{-1}, abs. corr. range: 0.888–0.954. 29392 Reflections were measured up to a resolution of (sin $\theta/\lambda)_{max}$ = 0.59 Å^{-1}. 7007 Reflections were unique (R_{int} = 0.0663), of which 4881 were observed [$I > 2\sigma(I)$]. 516 Parameters were refined with 57 restraints. $R1/wR2$ [$I > 2\sigma(I)$]: 0.0417/0.0925. $R1/wR2$ [all refl.]: 0.0686/0.0981. S = 0.988. Residual electron density found between −0.40 and 0.54 eÅ^{-3}.

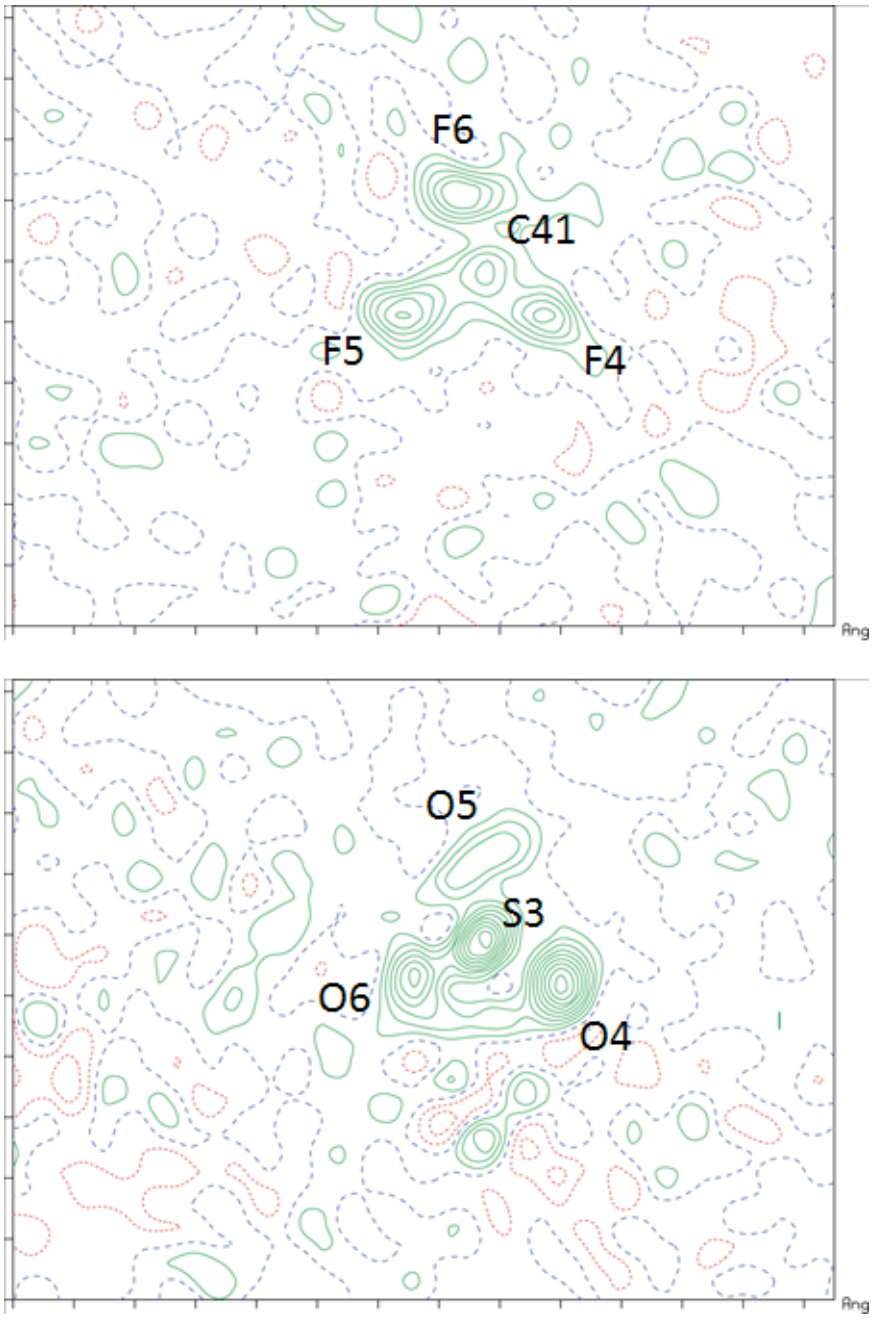

Figure S14. Electron-density coutour maps projected for the mean planes C41 F4 F5 F6 and S3 O4 O5 O6 for complex **2**.

Complex 7. The asymmetric unit of **7** contains one molecule of the Fe complex, two non-coordinated triflate counterions and one lattice dichloromethane molecule. The structure

of **7** is partly disordered. Both triflate counterions and the acetonitrile ligand are disordered. The occupancy factors of the major components of the disorder refine to 0.800(4), 0.666(4), 0.811(12), respectively. The structure is also found to be twinned racemically, and the BASF parameter refines to 0.500(14). Fw = 997.71, red irregularly shaped crystal, 0.44 × 0.19 × 0.11 mm^3, orthorhombic, $Pca2_1$ (no. 29), a = 16.9302(4), b = 11.4976(2), c = 24.1945(7) Å, V = 4709.62(19)$Å^3$, Z = 4, D_x = 1.407 g cm^{-3}, μ = 0.597 mm^{-1}, abs. corr. range: 0.848–0.940. 22859 Reflections were measured up to a resolution of $(\sin \theta/\lambda)_{max}$ = 0.59 $Å^{-1}$. 7944 Reflections were unique (R_{int} = 0.0426), of which 6218 were observed [$I > 2\sigma(I)$]. 722 Parameters were refined with 577 restraints. $R1/wR2$ [$I > 2\sigma(I)$]: 0.0381/0.0721. $R1/wR2$ [all refl.]: 0.0577/0.0759. S = 0.948. Residual electron density found between −0.41 and 0.32 $eÅ^{-3}$.

References

(1) Britovsek, G. J. P.; Bruce, M.; Gibson, V. C.; Kimberley, B. S.; Maddox, P. J.; Mastroianni, S.; McTavish, S. J.; Redshaw, C.; Solan, G. A.; Stromberg, S.; White, A. J. P.; Williams, D. J. *J. Am. Chem. Soc.* **1999,** *121*, 8728-8740.

(2) Britovsek, G. J. P.; England, J.; Spitzmesser, S. K.; White, A. J. P.; Williams, D. J. *Dalton Trans.* **2005**, 945-955.

(3) Evans, D. F.; Jakubovic, D. A. *J. Chem. Soc., Dalton Trans.* **1988**, 2927.

(4) P.T. Beurskens, G. Beurskens, R. de Gelder, S. Garcia-Granda, R.O. Gould, and J.M.M. Smits (2008). The DIRDIF2008 program system, Crystallography Laboratory, University of Nijmegen, The Netherlands.

(5) Sheldrick, G. M. *Acta Cryst.* **2008**, A64, 112-122.